ulator. The experimental results have validated the two control schemes and demonstrated that the redundancy can be effectively utilized to optimize various objective functions.

Our current research is focusing on theoretical analyses of the stability of the two control schemes and on developing some novel objective functions that can improve the performance of compliant motion.

Appendix

Initial configurations, feedback gains, and target impedances used in each experiment are as follows.

Figs. 3 and 4: $\boldsymbol{q}_0 = (83, -110, -64.5)^{T\circ}$, $\boldsymbol{K}_{xP} = diag(4000, 4000, 100)$, $\boldsymbol{K}_{xD} = diag(63, 63, 20)$, $\boldsymbol{K}_{fI} = diag(25, 25)$

Fig. 5: $\boldsymbol{q}_0 = (100, -120, -50)^{T\circ}$, $\boldsymbol{M} = diag(2, 1)$ Kg, $\boldsymbol{D} = diag(178, 89)$, $diag(178, 52)$ N $\cdot$ s/m, $\boldsymbol{K} = diag(4000, 2000)$, $diag(4000, 667)$ N/m, $\boldsymbol{K}_{yP} = 3000$, $\boldsymbol{K}_{yD} = 110$

Fig. 6: $\boldsymbol{q}_0 = (100, -120, -50)^{T\circ}$, $\boldsymbol{K}_{xP} = diag(1000, 1000, 3000)$, $\boldsymbol{K}_{xD} = diag(32, 32, 55)$, $\boldsymbol{K}_{fI} = diag(25, 25)$

Fig. 7: $\boldsymbol{q}_0 = (82, -110, -64.5)^{T\circ}$, $\boldsymbol{M} = diag(2, 1)$, $diag(2, 1)$ Kg, $\boldsymbol{D} = diag(178, 89)$, $diag(178, 52)$ N $\cdot$ s/m, $\boldsymbol{K} = diag(4000, 2000)$, $diag(4000, 667)$ N/m, $\boldsymbol{K}_{yP} = 100$, $\boldsymbol{K}_{yD} = 20$.

References

[1] M. H. Raibert and J. J. Craig, "Hybrid position/force control of manipulators," *ASME J. Dyn. Syst. Meas. Contr.*, vol. 102, pp. 126-133, 1981.

[2] N. Hogan, "Impedance control: An approach to manipulation, Part 1: Theory; Part 2: Implementation; Part 3: Applications," *ASME J. Dyn. Syst. Meas. Contr.*, vol. 107, pp. 1-24, 1985.

[3] M. T. Mason, "Compliance and force control for computer controlled manipulators," *IEEE Trans. Syst., Man, Cybern.*, vol. 11, pp. 418-432, 1981.

[4] D. E. Whitney, "Historic perspective and state of the art in robot force control," *Int. J. Robotics Res.*, vol. 6, pp. 3-14, 1987.

[5] O. Khatib, "A unified approach for motion and force control of robot manipulators: The operational space formulation," *IEEE J. Robotics Automat.*, vol. 3, pp. 43-53, 1987.

[6] T. Yabuta, A. J. Chona, and G. Beni, "On asymptotic stability of the hybrid position/force control scheme for robot manipulators," in *Proc. IEEE Int. Conf. Robotics Automat.*, 1988, pp. 338-343.

[7] C. H. An and J. M. Hollerbach, "The role of dynamical models in Cartesian force control of manipulators," *Int. J. Robotic Res.*, vol. 8, pp. 51-72, 1989.

[8] H. Kazerooni, T. B. Sheridan, and P. K. Houpt, "Robust compliant motion control for manipulators: Part 1: The fundamental concepts of compliant motion; Part 2: Design method," *IEEE J. Robotics Automat.*, vol. 2, pp. 83-105, 1986.

[9] N. Hogan, "Stable execution of contact tasks using impedance control," in *Proc. IEEE Int. Conf. Robotics Automat.*, 1987, pp. 1047-1054.

[10] Y. H. Chen and S. Pandey, "Uncertainty bounded-base hybrid control for robot manipulators," *IEEE Trans. Robotics Automat.*, vol. 6, pp. 303-311, 1990.

[11] T. Yoshikawa, "Dynamical hybrid position/force control of robot manipulators: Description of hand constraints and calculation of joint driving force," *IEEE J. Robotics Automat.*, vol. 3, no. 5, pp. 386-392, 1987.

[12] C. A. Klein and C. H. Huang, "Review of pseudoinverse control for use with kinematically redundant manipulators," *IEEE Trans. Syst., Man, Cybern.*, vol. 13, pp. 245-250, 1983.

[13] D. N. Nenchev, "Redundancy resolution through local optimization: A review," *J. Robotic Syst.*, vol. 6, pp. 769-798, 1989.

[14] J. Baillieul, "Avoiding obstacles and resolving kinematic redundancy," in *Proc. IEEE Int. Conf. Robotics Automat.*, 1986, pp. 1698-1704.

[15] R. V. Mayorga and A. K. C. Wong, "A singularities avoidance method for the trajectory planning of redundant robot manipulators," in *Proc. IEEE Int. Conf. Robotics Automat.*, 1987, pp. 1707-1712.

[16] J. M. Hollerbach and K. C. Suh, "Redundancy resolution of manipulators through torque optimization," *IEEE J. Robotics Automat.*, vol. 3, pp. 308-315, 1987.

[17] J. Baillieul, "Kinematic programming alternatives for redundant manipulators," in *Proc. IEEE Int. Conf. Robotics Automat.*, St. Louis, MO, 1985, pp. 722-728.

[18] P. H. Chang, "A close-form solution for inverse kinematics of robot manipulators with redundancy," *IEEE J. Robotics Automat.*, vol. 3, pp. 393-403, 1987.

[19] H. Seraji, "Configuration control of redundant manipulators: Theory and implementation," *IEEE J. Robotics Automat.*, vol. 5, pp. 472-490, 1989.

[20] L. Sciavicco and B. Siciliano, "A dynamic solution to the inverse kinematic problem for redundant manipulators," in *Proc. IEEE Int. Conf. Robotics Automat.*, 1987, pp. 1081-1087.

[21] W. S. Newman and M. E. Dohring, "Augmented impedance control: An approach to compliant control of kinematically redundant manipulators," in *Proc. IEEE Int. Conf. Robotics Automat.*, 1991, pp. 30-35.

[22] D. E. Whitney, "Resolved motion rate control of manipulators and human prosthesis," *IEEE Trans. Man-Machine Syst.*, vol. 10, pp. 47-53, 1969.

[23] J. Y. S. Luh, M. W. Walker, and R. P. C. Paul, "Resolved acceleration control of mechanical manipulators," *IEEE Trans. Automat. Contr.*, vol. 25, pp. 468-474, 1980.

[24] M. Avriel, *Nonlinear Programming: Analysis and Methods.* New York: Academic, 1971.

[25] T. Shamir and Y. Yomdin, "Repeatability of redundant manipulators: Mathematical solution of the problem," *IEEE Trans. Automat. Contr.*, vol. 33, pp. 1004-1009, 1988.

[26] T. Shamir, "Remarks on some dynamical problems of controlling redundant manipulators," *IEEE Trans. Automat. Contr.*, vol. 35, pp. 341-344, 1990.

[27] D. R. Baker and C. W. Wampler, "On the inverse kinematics of redundant manipulators," *Int. J. Robotics Res.*, vol. 7, no. 2, pp. 3-21, 1988.

[28] T. Yoshikawa, "Manipulability of robotic mechanisms," *Int. J. Robotics Res.*, vol. 4, pp. 3-9, 1985.

[29] Z. X. Peng, N. Adachi and S. Nakajima, "Extended hybrid position/force control of redundant robotic manipulators: Theory and implementation," *JSME Trans.*, vol. 57c, pp. 1273-1278, 1991 (in Japanese).

Exponential Control Law for a Mobile Robot: Extension to Path Following

O. J. Sørdalen and C. Canudas de Wit

***Abstract*—A piecewise smooth feedback control law for path following for the kinematic model of a nonholonomic mobile robot is proposed. The resulting motion can consist of stopping and reversing phases. The desired path is supposed to be composed of straight lines and arcs of circles joined at intermediate configurations. The proposed feedback control law yields exponential convergence to configurations representing stopping phases and to the terminal configuration.**

Manuscript received February 5, 1992; revised November 18, 1992. This work was supported in part by the Royal Norwegian Council for Scientific and Industrial Research (NTNF).

O. J. Sørdalen is with the Department of Engineering Cybernetics, The Norwegian Institute of Technology, 7034 Trondheim-NTH, Norway.

C. Canudas de Wit is with the Laboratoire d'Automatique de Grenoble, URA C.N.R.S. 228, ENSIEG-INPG, Grenoble, France.

IEEE Log Number 9212601.

1042-296X/93$03.00

I. Introduction

Feedback control strategies for mobile robots are important to compensate for disturbances and errors in the initial condition. The problems of path following or tracking and of stabilization about a constant configuration have been treated as separate problems for nonholonomic mobile robots. This is due to the nonexistence of smooth static-state feedback laws that stabilize the systems considered in [1] and [3], whereas nonlinear controllers for path following or tracking of nonstationary trajectories have been proposed by [6], [9], [10], and [12]. The requirement of nonstationary motion excludes the stabilization problem. The problem of the stabilization of a cart has been solved by using a smooth feedback law that also depended on the independent time variable as first proposed by [10]. This control scheme yields asymptotic stabilization about the origin with a maximum rate of $1/t$ for the system considered. An alternative to a time-dependent smooth controller is a discontinuous or a piecewise smooth controller. A piecewise smooth static-state feedback law that makes the cart globally *exponentially* converge to the origin with zero orientation was proposed in [2].

In this paper a unified approach is derived to make the kinematic model of a mobile robot globally follow a path with the possibility of stopping and reversing phases. With this approach for path following the problem of making the mobile robot converge to a constant configuration is solved as a special case of the path following problem. This paper extends the results in [2] to exponential convergence to an arbitrary configuration via a coordinate transformation. A feedback control law is then derived to make the cart follow a desired path that is supposed to be composed of straight lines and arcs of circles. Such a path is a result of several path planners and is easily represented as a sequence of positions and orientations. The shortest path between two configurations with the curvature upper bounded is also composed of straight lines and arcs of circles, in the case of no obstacles [4], [8]. The tracking error can be chosen to be arbitrarily small. Examples of this method and simulation results are presented.

II. Exponential Convergence to Arbitrary Configuration

The mobile robot considered here is a cart consisting of two independently actuated wheels connected by an axle. The kinematics of a cart is given by

$$\dot{q} = G(q)\begin{bmatrix} v \\ \omega \end{bmatrix}, \quad G(q) = \begin{bmatrix} \cos\theta & 0 \\ \sin\theta & 0 \\ 0 & 1 \end{bmatrix} \tag{1}$$

where the state of the system (1), $q = [x, y, \theta]^T$, is the position of the center of the axle (x, y) and the cart orientation θ with respect to the x axis. We assume that the tangential velocity v and the angular velocity ω can be regarded as the inputs to the system, i.e., $u = [v, \omega]^T$.

Let $q_r = [x_r, y_r, \theta_r]^T$ be a reference point in the configuration space. The control problem addressed in this section consists of designing a control law $u(q, q_r)$ so that the closed-loop system $\dot{q} = G(q)u(q, q_r) = f(q, q_r)$ converges for any initial condition $q(0)$, to an equilibrium point in $\mathcal{Q}$ where

$$\mathcal{Q} = \{(x, y, \theta) = (x_r, y_r, \theta_r + 2\pi n); \quad n = 0, \pm 1, \pm 2, \cdots\}.$$

The set $\mathcal{Q}$ thus represents a constant configuration in the configuration space $R^2 \times S^1$, which means that all points in $\mathcal{Q}$ are equivalent in terms of positioning and orienting the cart.

The exponential convergence to a given configuration will be obtained by using the piecewise smooth feedback law in [2] and [11] combined with a coordinate transformation. We introduce the error vector $q_e(t)$ as in [6],

$$q_e = [x_e, y_e, \theta_e]^T = T(\theta_r)(q - q_r) \tag{2}$$

$$T(\theta_r) = \begin{bmatrix} \cos\theta_r & \sin\theta_r & 0 \\ -\sin\theta_r & \cos\theta_r & 0 \\ 0 & 0 & 1 \end{bmatrix}. \tag{3}$$

The time derivative of q_e is given from (2) and (1),

$$\dot{q}_e = T(\theta_r)\dot{q} = T(\theta_r)G(q)u = G(q_e)u. \tag{4}$$

The convergence of q to an element in $\mathcal{Q}$ is equivalent to the convergence of q_e to an element in $\mathcal{O} = \{(x_e, y_e, \theta_e) = (0, 0, 2\pi n); n = 0, \pm 1, \pm 2, \cdots\}$.

Consider the following set $\mathcal{P}$:

$$\mathcal{P} = \{(x_e, y_e) \mid x_e^2 + (y_e - r)^2 = r^2\} \tag{5}$$

as the set of circles in the $x_e y_e$-plane with radius $r = r(x_e, y_e)$. They pass through the origin and (x_e, y_e) and are centered on the y_e axis with $\partial y_e/\partial x_e = 0$ in the origin. Let θ_d be the angle of the tangent of $\mathcal{P}$ at (x_e, y_e), defined as

$$\theta_d(x_e, y_e) = \begin{cases} 2\arctan(y_e/x_e); & (x_e, y_e) \neq (0, 0) \\ 0; & (x_e, y_e) = (0, 0). \end{cases} \tag{6}$$

θ_d is taken by convention to belong to $(-\pi, \pi]$. Hence θ_d has discontinuities on the y_e axis with respect to x_e. We then introduce the following functions:

$$a(x_e, y_e) = r\theta_d = \frac{x_e^2 + y_e^2}{y_e}\arctan(y_e/x_e) \tag{7}$$

$$\alpha(x_e, y_e, \theta_e) = e - 2\pi n(e), \; e = \theta_e - \theta_d \tag{8}$$

where a is the arc length, and the orientation error $\alpha \in (-\pi, \pi]$ is a periodic and piecewise continuous function with respect to e. The variable n takes values in $\{0, \pm 1, \pm 2, \cdots\}$ so that α belongs to $(-\pi, \pi]$. The angle α is introduced so that all the elements in $\mathcal{O}$ are mapped into the unique point $(a, \alpha) = (0, 0)$. Note that $a(x_e, y_e)$ defines the arc length from the origin to (x_e, y_e) along a circle that is centered on the y_e axis and passes through these two points. The function $a(x_e, y_e)$ may be positive or negative according to the sign of x_e. When $y_e = 0$, we define $a(x_e, 0) = x_e$, which makes $a(x_e, y_e)$ continuous with respect to y_e since $a(x_e, \epsilon) \approx x_e$ when $\epsilon \approx 0$. Discontinuities in $a(x_e, y_e)$ only take place on the y_e axis. An illustration of these definitions is shown in Fig. 1.

We introduce the function $F(\cdot)$: $R^3 \to R \times (-\pi, \pi]$ as in [2], mapping the state space coordinates $q_e \in R^3$ into the two-dimensional space $z \in R \times (-\pi, \pi]$

$$z = F(q_e); \qquad F(q_e) = \begin{bmatrix} a(x_e, y_e) \\ \alpha(x_e, y_e, \theta_e) \end{bmatrix} \tag{9}$$

where $F(0) = 0$.

We introduce the set

$$\Psi = R^3 - (\mathcal{D}_0 \cup \mathcal{E}_0)$$

where $\mathcal{D}_0 = \mathcal{D} \cup \{q \mid x_e = y_e = 0\}$ and $\mathcal{E}_0 = \mathcal{E} \cup \{q \mid x_e = y_e = 0\}$, and

$$\mathcal{D} = \{q \mid x_e = 0, y_e \neq 0\}$$

$$\begin{aligned} \mathcal{E} &= \{q \mid \alpha(x_e, y_e, \theta_e) = -\pi\} \\ &= \{q \mid \theta = \theta_d(x_e, y_e) + 2\pi n - \pi\}, \qquad n \in \{0, \pm 1, \pm 2, \cdots\}. \end{aligned}$$

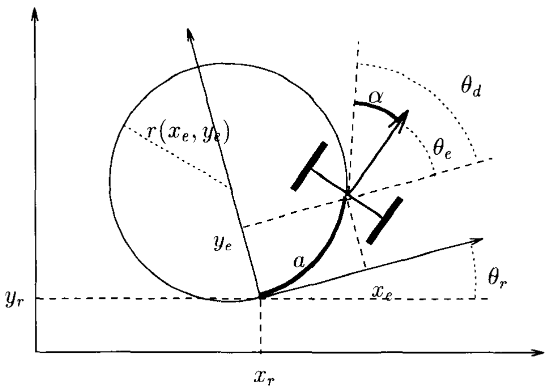

Fig. 1. Illustration of the coordinate system.

In the domain Ψ where $F(\cdot)$ is differentiable, i.e., $q_e \in \Psi$, we have

$$\dot{z} = J(q_e)\dot{q}_e \tag{10}$$

where $J(q_e) = \partial F/\partial q_e \in R^{2\times 3}$. Equation (4) then gives

$$\dot{z} = J(q_e)G(q_e)u = B(q_e)u; \qquad B = \begin{bmatrix} b_1 & 0 \\ b_2 & 1 \end{bmatrix} \tag{11}$$

where

$$b_1 = \cos\theta_e\left(\frac{\theta_d}{\beta} - 1\right) + \sin\theta_e\left(\frac{\theta_d}{2}\left(1 - \frac{2}{\beta^2}\right) + \frac{1}{\beta}\right) \tag{12}$$

$$b_2 = \cos\theta_e\frac{2\beta}{(1+\beta^2)x_e} - \sin\theta_e\frac{2}{(1+\beta^2)x_e} \tag{13}$$

where $\beta = y_e/x_e$. Taking the following control law, as in [2], with $\gamma > 0$ and $k > 0$,

$$v = -\gamma b_1 a \tag{14}$$

$$\omega = -b_2 v - k\alpha = \gamma b_1 b_2 a - k\alpha \tag{15}$$

gives the closed-loop equations:

$$\begin{aligned} \dot{a} &= b_1 v = -\gamma b_1^2 a \\ \dot{\alpha} &= b_2 v + \omega = -k\alpha. \end{aligned} \tag{16}$$

It is shown in [2] that b_1 converges to 1 as α converges to 0. In the same way as in [2] and [11], with a discussion of discontinuities, we can state the exponential convergence of the q_e-trajectories to any of the members of $\mathcal{O}$ and the control inputs $v(q_e)$ and $\omega(q_e)$ remain bounded.

Fig. 4 shows the resulting paths in the xy-phase plane for several initial conditions corresponding to different points on the unit circle with an initial orientation angle $\theta(0) = \pi/2$. We see that all these phase trajectories converge to the origin by asymptotically tracking one of the circles in the path family $\mathcal{P}$. The constants k and γ were chosen to be 4.60 and 1.35, respectively.

Remark: We have assumed that the mobile robot can be modeled with velocity inputs. This means that the dynamics from the torque to the velocity input is neglected. The control law introduced in this paper may introduce discontinuities in the velocity inputs. These velocity inputs can be regarded as references for the real velocities that are controlled by the torques. Physically the real velocities cannot exactly follow the discontinuous references. The effects of this approximation can be neglected or important depending on the physical system and can be a topic for future research.

III. Tracking a Sequence of Points

In this section we extend the results from the preceding section to track a sequence of points in the configuration space. The problem is not to regulate the cart about one point, rather to make the cart move from one point in the configuration space to another by using feedback combined with some path planning. In environments with obstacles, it is customary to define a certain number of intermediate points between the initial point p_1 and final point p_n so that the obstacles can be avoided. Suppose that a path planner gives a path that is composed of arcs of circles and straight lines joined in the points $p_2, p_3, \cdots, p_{n-1}$ given by the sequence $p = (p_1, p_2, \cdots, p_n)$. An element p_i is a point defined in the configuration space, i.e., given by a position (x_i, y_i) and an orientation θ_i

$$p_i = [x_i, y_i, \theta_i]^T.$$

The existence of a path composed of arcs of circles and straight lines was discussed in [7]. The problem of how to optimally choose the intermediate points is, however, not yet completely solved. In the case of no obstacles the shortest path with the curvature upper bounded is composed of arcs of circles and straight lines [4], [8], [5].

Note that each point p_i represents a local coordinate system, each with a set of circles as defined in (5), $\mathcal{P}_i$, associated with it. We associate each point p_i with a desired velocity v_i and a maximum deviation ϵ_i from p_i before switching to p_{i+1} as the new point of attraction. We define the vector ϵ as the vector consisting of the maximum deviations, $\epsilon = [\epsilon_1, \epsilon_2, \cdots, \epsilon_{n-1}]^T$ where $\epsilon_i > 0$, and the vector V as the vector consisting of the desired velocities, $V = [v_1, v_2, \cdots, v_{n-1}]^T$.

We can change between forward and backward motion by separating positive and negative velocities with a zero velocity. From p_i and p_{i+1} it is easy to calculate the arc length between these two points. We denote this length by d_i, which is given by $d_i = a(x_i^{i+1}, y_i^{i+1})$, where a is the arc length as defined by (7). The point (x_i^{i+1}, y_i^{i+1}) is the position (x_i, y_i) transformed to the coordinate system defined by p_{i+1}. Thus d_i can be positive or negative. We define the vector d as the vector consisting of these lengths, $d = [d_1, d_2, \cdots, d_{n-1}]^T$. We assume that the desired path from p_i to p_{i+1} does not cross the y axis defined by p_{i+1}. This can easily be satisfied by adding another intermediate point between p_i and p_{i+1}. We change to p_{i+1} as the new point of attraction when $|a| < \epsilon_i$. The index function I is thus given by

$$I = \begin{cases} 1, & \text{when } t = 0 \\ I + 1, & \text{when } |a| \le \epsilon_I \end{cases}.$$

The desired circles are made stable by a feedback law as in Section II:

$$\omega = -b_2 v - k\alpha. \tag{17}$$

The orientation error α is then given by

$$\dot{\alpha} = -k\alpha. \tag{18}$$

This implies that $\alpha(t)$ converges exponentially to zero implying that the motion converges towards a motion along one of the circles that pass through the actual reference configuration. This situation is illustrated in Fig. 2, where we see that the circles define a kind of funnel towards each point p_i along the desired path. From [2] we have that b_1 converges to 1 as α converges to zero. This means that $\dot{a}$ converges asymptotically to v according to (16). The input v can be chosen to interpolate between the desired velocities v_i in many different ways. Here we choose a control law that gives a

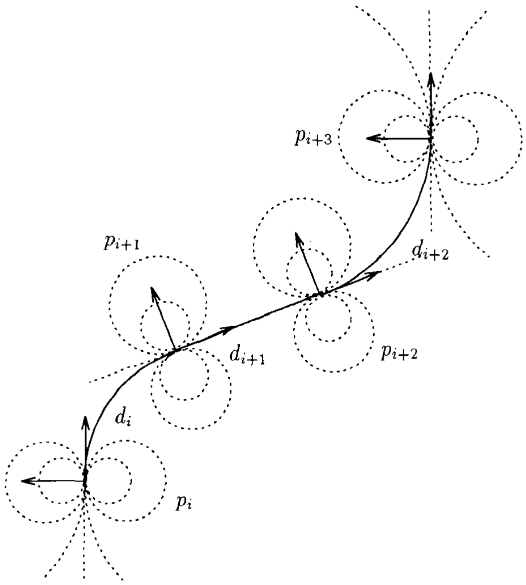

Fig. 2. Illustration of the circles defined by the points p_i.

continuous $v(t)$ and $\dot{v}(t) = 0$ when changing from one point of attraction to another:

$$v(t^i_-) = v(t^i_+) = v_{i-1}, \quad \dot{v}(t^i_+) = 0.$$

Here, t^i is the instant of time when the index function I increments from $i - 1$ to i.

Since the desired path from p_{i-1} to p_i does not cross the y axis defined by p_i, the sign of d_{i-1} is the opposite of the sign of v_{i-1} and v_i. v_{i-1} and v_i cannot have opposite signs, but one of these velocities can be zero, for instance, in order to change between forward and backward motion. The tangential velocity $v(t)$ in (14) is thus modified to account for the velocity requirements when $1 < i < n$ and $\tau \in [0, \tau_f]$ as follows:

$$v(\tau) = v_{i-1} + 3\Delta v \left(\frac{\tau}{\tau_f}\right)^2 - 2\Delta v \left(\frac{\tau}{\tau_f}\right)^3 \tag{19}$$

where

$$\tau_f = -\frac{2d_{i-1}}{v_{i-1} + v_i}, \qquad \Delta v = v_i - v_{i-1}. \tag{20}$$

τ is the time variable that is reset to zero when the index function I increments. τ_f is the time it takes to reach p_i along the desired circle if the cart is exactly at p_{i-1} at $\tau = 0$, if the input $v(\tau)$ is given by (19). Because of possible disturbances or model errors the time needed to reach p_i may be different from τ_f. If the time needed is shorter than τ_f, then the index function I increments when the cart reaches the neighborhood of p_i, and τ is reset to zero. Note that because of the exponential convergence of the orientation to the angle $\theta_d(x_e, y_e)$ given by the tangent of the actual circle, the cart has to pass through the neighborhood of p_i. Therefore the cart cannot "overshoot" this neighborhood without switching to p_{i+1} as the new point of attraction. If the time needed is longer than τ_f, then the control law has to ensure that the cart reaches the neighborhood of the point p_i. To this end we let the velocity be continuous equal to v_i during the time $\mathfrak{Z}$ after t_f. If the cart has not reached the neighborhood of p_i after time $\tau_f + \mathfrak{Z}$, then we let the cart converge to p_i with a feedback law as in Section II:

$$v(\tau) = \begin{cases} v_i, & \tau \in (\tau_f, \tau_f + \mathfrak{Z}] \\ -\gamma b_1 a, & \tau > \tau_f + \mathfrak{Z}. \end{cases} \tag{21}$$

This ensures that the cart will reach the neighborhood of p_i in finite time.

When $i = 1$, v is given by a feedback law in order to converge to the starting point p_1,

$$v(t) = -\gamma b_1 a(1 - e^{-\lambda t}) \tag{22}$$

where γ and λ are positive constants. This results in $v(0) = 0$. It is natural to choose the starting velocity of the path v_0 equal to zero. In that case, $v(t)$ will converge to this velocity. The closed-loop equation is

$$\dot{a} = -\gamma b_1^2 a(1 - e^{-\lambda t}). \tag{23}$$

From (18) and [2] we have that b_1 converges to 1. This implies that there exists a positive constant ϵ and a finite time T such that $\gamma b_1^2(1 - e^{-\lambda t}) > \epsilon$ for all $t > T$. Equation (23) gives that $a(t)$ converges to zero and $|a(t^1)| < \epsilon_1$ for some finite t^1.

At the end of the desired path, i.e., $i = n$, we want the cart to exponentially converge to p_n. To make $\dot{v}(t)$ continuous, we propose the following feedback law:

$$v = -b_1 \gamma a(1 - \delta e^{-\lambda \tau}) \tag{24}$$

where γ, λ, and δ are positive constants. To have $v(0)$ and v_{n-1} and $\dot{v}(0) = 0$ when $b_1 = 1$, we choose

$$\delta = 1 + \frac{v_{n-1}}{d_{n-1}\gamma}, \quad \lambda = \frac{v_{n-1}^2}{(d_{n-1}\gamma + v_{n-1})d_{n-1}}, \quad \gamma > -\frac{v_{n-1}}{d_{n-1}}.$$

Note that $v_{n-1}/d_{n-1} < 0$ by assumption so that $\delta < 1$. This gives the closed-loop equation:

$$\dot{a} = -b_1^2 \gamma a(1 - \delta e^{-\lambda \tau}). \tag{25}$$

As in the case $i = 1$, a will be asymptotically stable about zero. If $b_1 = 1$, then the solution of (25) is

$$a(t) = a(0) \exp\left(-\left\{\gamma t + \frac{\gamma\delta}{\lambda}(1 - e^{-\lambda t})\right\}\right). \tag{26}$$

More generally, v_i may be a function of time and the arc length a in order to let the cart stand still at the point p_{i-1} for a certain time. If we want the cart to stand still at p_{i-1} during the time T, we can choose $v_{i-1} = 0$ and v_i as follows:

$$v_i = \begin{cases} 0, & t < t^i + T \\ \nu, & t \geq t^i + T \end{cases}$$

where t^i is the point of time when $|a|$ becomes less than ϵ_{i-1} and ν is the velocity with which we want the cart to leave p_{i-1}. This velocity can be positive or negative, and may be a function of time. Hence, with *this* approach it is possible to follow a path where the cart can stop, drive forward or backward by defining p and V accordingly. It remains to show that the inputs remain bounded.

Theorem 1: The control law defined by (19) and (17) implies that the inputs $v(t)$ and $\omega(t)$ remain bounded.

Proof: b_1 is bounded from [2]. From (23) and (25), we have that a remains bounded. With v_{i-1} (and v_i) finite, (19), (21), and (22) show that $v(t)$ will remain bounded. Since α is bounded by definition, ω will remain bounded if $b_2 v$ is bounded. We find with

$\beta = y_e/x_e$:

$$
\begin{aligned}
|b_2(q_e)v| &= \left|\cos\theta_e \frac{2\beta}{(1+\beta^2)x_e} - \sin\theta_e \frac{2}{(1+\beta^2)x_e}\right| |v| \\
&\le \frac{2}{x_e^2 + y_e^2}\sqrt{x_e^2 + y_e^2}\,|v| \\
&= \frac{2|v|}{\sqrt{x_e^2 + y_e^2}} \le \frac{4|v|}{\pi |a|} \le \frac{4\max\{|v_{i-1}|, |v_i|\}}{\pi \min\{\epsilon_i\}}.
\end{aligned}
$$

□

Here, we have used the fact that $|a| \le (\pi/2)\sqrt{x_e^2 + y_e^2}$, and that the point of attraction changes from p_{i-1} to p_i when $|a| = \epsilon_i$ so that $|a| \ge \min\{\epsilon_i\} > 0$. From (19) we have that $|v| \le \max\{|v_{i-1}|, |v_i|\}$. This proof shows that $|b_2(q_e)v|$ can be arbitrarily bounded by choosing ϵ_i, v_{i-1}, and v_i appropriately.

We have shown that the proposed control law makes the cart reach the neighborhood of every point p_i where the neighborhood is given by ϵ_i. The exponential convergence of $\alpha(t)$ to zero can be used to show that the cart stays in the neighborhood of the desired nominal circle segment between the intermediate points p_i and p_{i+1}. The motion of the cart at a point (x_e, y_e) can be decomposed in a motion tangential to the actual circle representing the desired motion, and in a motion perpendicular to the desired motion resulting in a deviation from the actual circle. Let the deviation of the cart from the nominal circle segment be denoted by ρ. The sign of ρ is defined so that a positive orientation error α results in a positive derivative $\dot{\rho}$ in forward motion. We introduce the integral

$$
I_\rho = \int_0^t v(\tau)\sin\alpha(\tau)\,d\tau + \epsilon_i
$$

where $v(\tau)$ is the velocity of the cart, ϵ_i is the maximal deviation from the last point of attraction p_i, and $\alpha(\tau)$ is the orientation error of the cart with respect to the tangent of the actual circle. The time t is set to zero when the cart reaches the neighborhood of p_i and p_{i+1} becomes the new point of attraction. The integral I_ρ represents a distance from the nominal circle segment along a path perpendicular to the circles in the set $\mathcal{P}$. The circles in the family $\mathcal{P}$ become denser as the cart moves toward the point p_{i+1}. This situation is illustrated in Fig. 3.

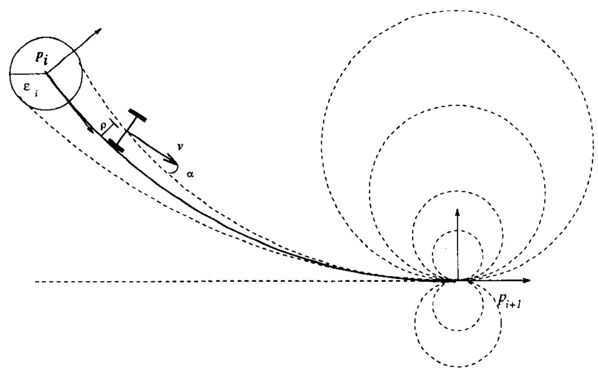

Fig. 3. An illustration of the motion of the cart in the neighborhood of the nominal path between p_i and p_{i+1}.

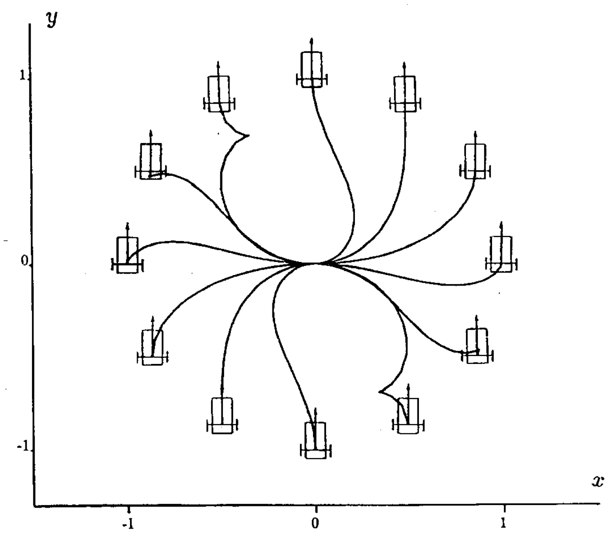

Fig. 4. Resulting paths when the cart is initially on the unit circle in the xy-plane with $\theta(0) = \pi/2$.

Because of this property of $\mathcal{P}$ we see from a geometrical point of view that

$$
|\rho(t)| \le |I_\rho| \le \left|\int_0^t v(\tau)\sin\alpha(\tau)\,d\tau\right| + \epsilon_i. \tag{27}
$$

From (18) we find $\alpha(t) = \alpha(0)e^{-kt}$. We define $v_{mi} = \max\{v_i, v_{i+1}\}$. Equation (27) thus implies

$$
\begin{aligned}
|\rho(t)| &\le v_{mi}\left|\int_0^t \sin(\alpha(0)e^{-k\tau})\,d\tau\right| + \epsilon_i \\
&\le v_{mi}\left|\int_0^t \alpha(0)e^{-k\tau}\,d\tau\right| + \epsilon_i \\
&\le \frac{v_{mi}}{k}|\alpha(0)e^{-k\tau} - \alpha(0)| + \epsilon_i \le \frac{2v_{mi}}{k}|\alpha(0)| + \epsilon_i.
\end{aligned}
$$

We see that by choosing k, $v_{mi} = \max\{v_i, v_{i+1}\}$, and ϵ_i appropriately, the resulting path of the cart will stay arbitrarily close to the nominal path between the points p_i and p_{i+1}.

As an example of this approach, we want the cart to pass through a corridor with a corner. The points p_i were chosen as follows:

$$
\begin{aligned}
p_1 &= \left[1, 1, \frac{\pi}{2}\right]^T, \quad p_2 = \left[1, 2, \frac{\pi}{2}\right]^T, \\
p_3 &= [2, 3, 0]^T, \quad p_4 = [4, 3, 0]^T, \\
p_5 &= \left[5, 2, -\frac{\pi}{2}\right]^T, \quad p_6 = \left[5, 1, -\frac{\pi}{2}\right]^T.
\end{aligned}
$$

This results in the distance vector $d = [-1, -(\pi/2), -2, -(\pi/2), -1]^T$. The velocities were chosen to $V = [0, 0.5, 0.5, 0.5, 0.5]^T$. The accuracy vector ϵ and the initial state were chosen to $\epsilon = [0.001, 0.01, 0.01, 0.01, 0.01]^T$ and $q_0 = [0.9, 0.9, 0.5]^T$, respectively. The controller parameters k and γ were chosen to 2 and 2, respectively. A simulation was done in SIMNON. The resulting path in the xy-plane is shown in Fig. 5. Initially there is a transient phase to reach p_1. Thereafter the cart follows the desired path. This is due to being the points p_i chosen so that the resulting path consists of arcs of circles and straight lines. The position (x_i, y_i) defines a specific circle in the coordinate system of p_{i+1}. The position (x_i, y_i) also defines a desired angle, $\theta_d(x_i, y_i)$, corresponding to the angle of the tangent of this circle. The reference orientation θ_i is cho-

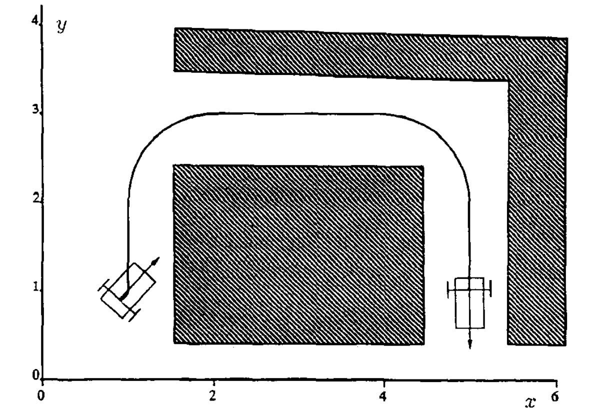

Fig. 5. The resulting path in the xy-plane when the cart passes through a corridor. The desired path is defined by the endpoints of the straight lines and the circle segment.

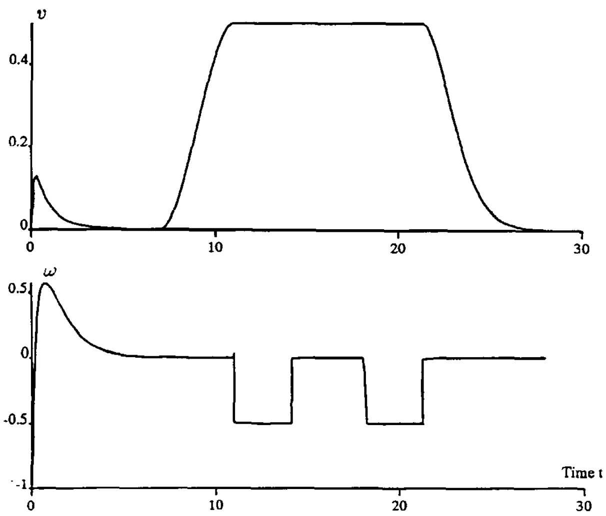

Fig. 6. Timeplots of the tangential velocity v and the angular velocity ω when the cart passes through a corridor.

sen to be equal to this angle, $\theta_d(x_i, y_i)$. Therefore, when the cart arrives in the neighborhood of p_i and we switch to p_{i+1} as the new point of attraction, the cart has already the desired orientation, i.e., $\alpha = 0$, and the arc of the circle from p_i to p_{i+1} becomes invariant. From Fig. 6 we see that the tangential velocity $v(t)$ is continuous and obtains the desired values. The angular velocity $\omega(t)$ is discontinuous when the path changes between a circle and a straight line as a result of the discontinuity in the curvature of such a path.

IV. Conclusion

A piecewise smooth controller has been presented for a mobile robot with two degrees of freedom. The cart exponentially converges to a position in the xy-plane with a desired orientation for any initial condition. This is achieved by letting the motion of the cart converge to one of the circles that pass through the origin and are centered on the y axis in a local coordinate system. An extension to the case of following a path composed of straight lines and arcs of circles has been proposed. This approach allows for stopping and reversing phases. The degree of accuracy can be arbitrarily chosen. Desired velocities at certain points along the path are to be specified and can be zero, positive, or negative. Therefore, stopping and reversing phases can be included by specifying the desired velocities accordingly. The convergence to the terminal configuration is exponential. Simulation results showed that the desired path was followed and the desired velocities were achieved. Different velocity profiles can be chosen by changing the structure of the control law for the tangential velocity v. An extension to other types of path segments than arcs of circles to have smoother transitions between the path segments can be a topic for further research.

References

[1] R. W. Brockett, "Asymptotic stability and feedback stabilization," in *Differential Geometric Control Theory*, R. W. Brockett, R. S. Millman and H. J. Sussman, Eds. Boston: Birkhauser, 1983, pp. 181-208.

[2] C. Canudas de Wit and O. J. Sørdalen, "Exponential stabilization of mobile robots with nonholonomic constraints," *IEEE Trans. Automat. Cont.*, vol. 37, pp. 1791-1797, Nov. 1992.

[3] G. Campion, B. d'Andrea-Novel, and G. Bastin, "Controllability and state feedback stabilizability of nonholonomic mechanical systems," in *Advanced Robot Control*, C. Canudas de Wit, Ed. New York: Springer-Verlag, 1991, pp. 106-124.

[4] L. Dubins, "On curves of minimal length with a constraint on average curvature and with prescribed initial and terminal positions and tangents," *Amer. J. Mathemat.*, vol. 79, pp. 497-516, 1957.

[5] Y. Kanayama and B. I. Hartman, "Smooth local path planning for autonomous vehicles," in *Proc. IEEE Conf. Robotics Automat.*, Scottsdale, AZ, May 1989, pp. 1265-1270.

[6] Y. Kanayama, V. Kimura, F. Miyazaki, and T. Noguchi, "A stable tracking control method for an autonomous mobile robot," in *Proc. IEEE Conf. Robotics Automat.*, Cincinnati, OH, 1990, pp. 384-389.

[7] J.-P. Laumond and T. Siméon, "Motion planning for a two degrees of freedom mobile robot with towing," in *Proc. IEEE Int. Conf. Control Applicat.*, 1989.

[8] J. A. Reeds and L. A. Shepp, "Optimal paths for a car that goes both forwards and backwards," *Pacific J. Mathemat.*, vol. 145, pp. 367-393, 1990.

[9] C. Samson and K. Ait-Abderrahim, "Feedback control of a nonholonomic wheeled cart in Cartesian space," in *Proc. IEEE Conf. Robotics Automat.*, Sacramento, CA, Apr. 1991, pp. 1136-1141.

[10] C. Samson, "Velocity and torque feedback control of a nonholonomic cart," in *Advanced Robot Control*, C. Canudas de Wit, Ed. New York: Springer-Verlag, 1991, pp. 125-151.

[11] O. J. Sørdalen, "Feedback control of nonholonomic mobile robots," Ph.D. dissertation, ITK-rapport 1993:5-W, The Norwegian Instit. Technol., Feb. 1993.

[12] G. Walsh, D. Tilbury, S. Sastry, R. Murray, and J. P. Laumond, "Stabilization of trajectories for systems with nonholonomic constraints," in *Proc. IEEE Conf. Robotics Automat.*, Nice, France, May 1992, pp. 1999-204.

Direct Kinematics of Parallel Manipulators

J.-P. Merlet

***Abstract*—The determination of the direct kinematics of fully parallel manipulators is in general a difficult problem but has to be solved for any practical use. Various methods are presented to solve this problem: two kinds of iterative schemes, a reduced iterative scheme, and a polynomial method. The computation time of these methods are compared and their various advantages are shown.**

Manuscript received August 2, 1989; revised May 22, 1992.

The author is with the Centre de Sophia-Antipolis, INRIA, 06902 Sophia Antipolis cedex, France.

IEEE Log Number 9212595.